Bulletin of the Seismological Society of America, Vol. 72, No. 5, pp. 1567–1590, October 1982

CRUSTAL STRUCTURE OF THE DIABLO AND GABILAN RANGES, CENTRAL CALIFORNIA: A REINTERPRETATION OF EXISTING DATA

By Allan W. Walter and Walter D. Mooney

ABSTRACT

The compressional-wave velocity structure of the crust of the Coast Ranges of central California was modeled from seismic refraction data reported previously. For both the Diablo Range (east of the San Andreas fault) and the Gabilan Range (west of the fault), two alternative velocity models were derived for each range by iterative two-dimensional ray tracing. Each pair of models shows a sedimentary layer and an underlying crust composed of three or four layers. For the Diablo Range, the velocities in the sediments range from 2.9 to 4.8 km/sec, and the depth to basement varies from 0.2 km within the central Diablo Range to a maximum of 3.4 km north of the Livermore Valley. In the Gabilan Range, the velocities in the sediments overlying the granitic basement are higher north of the Gabilan Range (3.6 to 4.6 km/sec) than to the south (2.2 to 3.8 km/sec), and the depth to basement both north and south of the range is less than 2 km.

Below the sediments and fractured near-surface material, a resolvable difference in the crustal velocity structure on opposite sides of the San Andreas fault indicates compositional differences at depth. The upper crust has an average velocity of 5.7 km/sec at depths between 3 and 16 ± 3 km in the Diablo Range and an average velocity of 6.1 km/sec at depths between 2 and 9 ± 1 km in the Gabilan Range. The lower crust has an average velocity of 6.9 km/sec at depths between 16 ± 3 and 30 km in the Diablo Range and an average velocity of 6.5 km/sec at depths between 10 and 24 km in the Gabilan Range. The models also show that the depth to Moho differs by several kilometers between the two ranges. In the Diablo Range models, the crust-mantle boundary becomes shallower from south to north, rising from a depth of 30 to 26 km. In the Gabilan Range models, the Moho is at a depth of 24 to 26 km, depending on the velocity assumed at the base of the crust.

Laboratory measurements of rock velocities and the mapped surface geology allow us to interpret the velocity models in terms of crustal composition. We conclude that the Diablo Range probably consists largely of metagraywacke to a depth of 16 ± 3 km, and gabbroic material below this depth. The crust of the Gabilan Range probably consists of granitic material to a depth of 9 ± 1 km and gneissic material below this depth. Franciscan rocks are not regionally present in the crust of the Gabilan Range. If the gneissic lower crust consists of the same rocks as are found at the surface in the Gabilan Range, then the presumed large-scale lateral motion of the Salinian block has taken place at or below the crust-mantle boundary, rather than along a mid-crustal slip plane.

Introduction

The compressional-wave velocity at depth of the individual geologic units that make up the Coast Ranges of central California is of particular interest because the Coast Ranges are the host rocks for the San Andreas fault system north of the Transverse Ranges of southern California. A knowledge of the crustal velocity structure along and across the fault can be used to locate and model earthquakes and to constrain the interpretation of gravity, magnetic, and heat flow anomalies. Furthermore, a knowledge of the structure of the Coast Ranges, which includes a post-Jurassic accretionary melange, is important to gaining an understanding of the origin and evolution of the Western United States.

Between San Francisco and the Transverse Ranges to the south, the Coast Ranges of central California consist of three major geologic units: the Diablo Range; the Salinian block; and the Sur-Obispo terrane located west of the Nacimiento fault zone (Figure 1). To measure the velocity-depth structure of Coast ranges on either

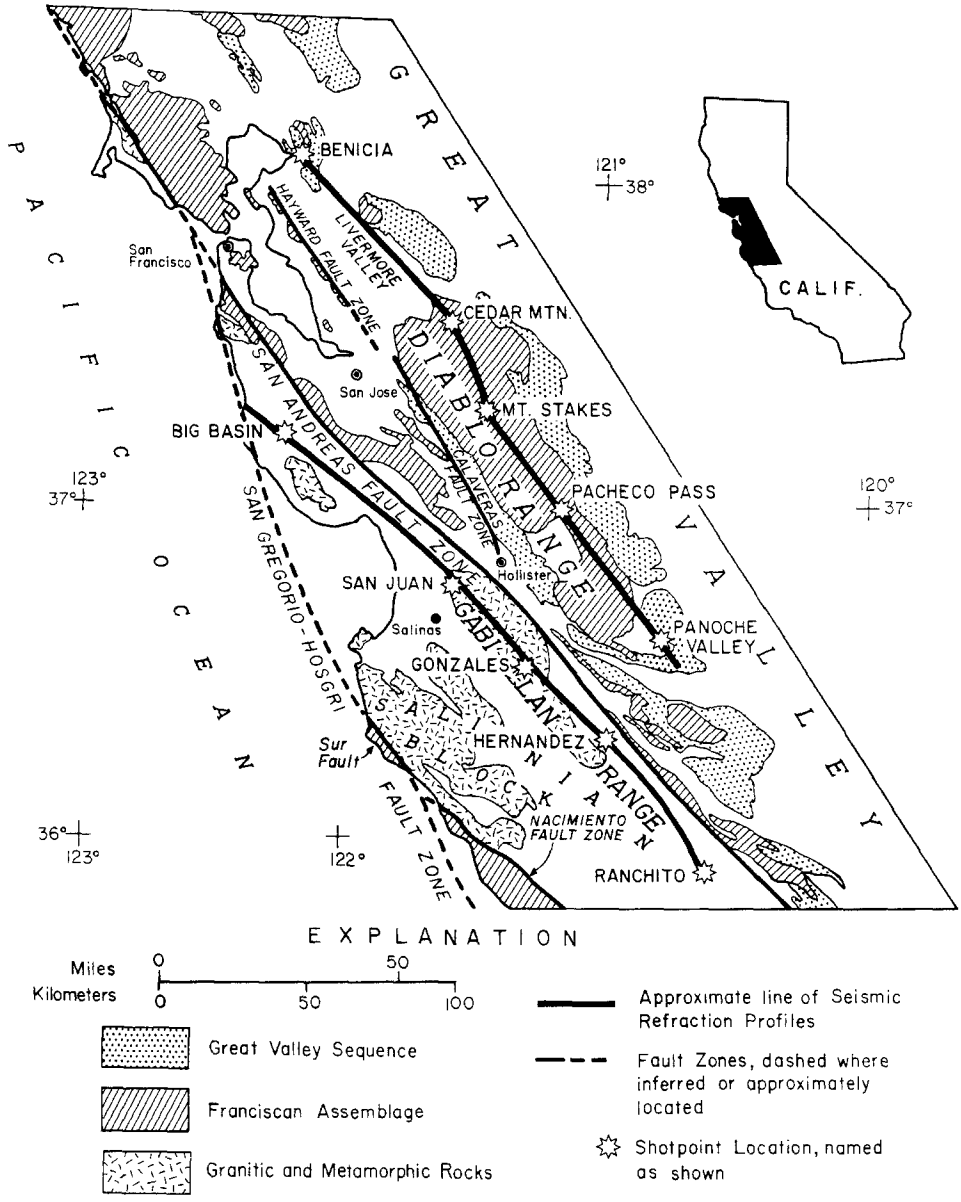

FIG. 1. Generalized geologic map of central California showing the locations of the Diablo Range and Gabilan Range profiles, modified from Stewart (1968). For the Diablo Range profile, the shotpoints are Benicia, Cedar Mountain, Mt. Stakes, Pacheco Pass, and Panoche Valley. For the Gabilan Range profile, the shotpoints are Big Basin, San Juan, Gonzales, Hernandez, and Ranchito.

side of the San Andreas fault, the United States Geological Survey (USGS) conducted two seismic refraction surveys in June 1967: the Diablo Range profile and the Gabilan Range profile. These profiles were analyzed in part by Stewart (1968). In this paper, we reinterpret the 1967 data using two-dimensional ray-tracing techniques, and we relate the resulting compressional-wave velocity structures to

laboratory measurements of ultrasonic velocities of a variety of rock types in order to infer crustal composition at depth. We present here new interpretations of the crustal structure of the Diablo Range and the easternmost side of the Salinian block, the Gabilan Range.

The Diablo Range is an antiformal structure that has an exposed core of the Mesozoic Franciscan assemblage virtually encircled by the Great Valley sequence (Figure 1). Despite their similarity in age and bulk composition, the Franciscan assemblage and the Great Valley sequence differ greatly in depositional histories. Although the Great Valley sequence shows regular bedding in normal stratigraphic sequence, the Franciscan assemblage is largely a melange of metasedimentary and volcanic rocks, which has led to the suggestion that it was deposited as an accretionary prism associated with a subduction zone, forearc basin, and volcanic arc (Dickinson, 1970).

The Diablo Range profile, east of the San Andreas fault, extends southeast from Benicia, across the Livermore Valley, and down the axis of the Diablo Range to the Panoche Valley (Figure 1). The five shotpoints along this profile are (north to south): Benicia; Cedar Mountain; Mt. Stakes; Pacheco Pass; and Panoche Valley. Between the Benicia and Cedar Mountain shotpoints, the profile crosses a variety of sedimentary rocks ranging in age from Late Cretaceous to Holocene (Rogers, 1966). South of Cedar Mountain and nearly to Panoche Valley, the profile is entirely within the Franciscan assemblage of the Diablo Range.

The Salinian block is bounded on the east by the San Andreas fault and on the west by the Sur and Nacimiento fault zones (Figure 1). The basement of the Salinian block consists of plutonic rocks locally overlain by Tertiary marine sedimentary rocks. The plutonic rocks, ranging in composition from tonalite to granite, have been intruded into metasedimentary rocks of largely amphibolitic grade (Ross and McCulloch, 1979). Because of the similarity in composition and age to parts of the Sierra Nevada batholith, several investigators (e.g., Page, 1980) have suggested that the Salinian block was originally positioned between the Sierra Nevada and the Peninsula Ranges of southern California; to assume its present position, as much as 540 km of lateral motion of the Salinian block was presumed to have occurred mainly on the San Andreas fault. Recent paleomagnetic studies (Champion *et al.*, 1980) have suggested an even more exotic origin for the Salinian block with movements of as much as 2500 km. The validity of these paleogeographic reconstructions is not the subject of this paper; however the hypothesis of great lateral movement raises the possibility that the plutonic rocks of the Salinian block are not rooted to the lower crust but have decoupled along a slip plane and been thrust over rocks of a different composition.

The Gabilan Range profile lies in the northern part of the Salinian block and extends southeast from the southern Santa Cruz Mountains, across the upper Salinas Valley, and down the axis of the range, where it terminates 13 km west of Parkfield (Figure 1). The five shotpoints along the profile are (north to south): Big Basin; San Juan; Gonzales; Hernandez; and Ranchito. The center three shotpoints are within the granite basement of the range. North of the range, between the San Juan and Big Basin shotpoints, the profile crosses continental and marine sediments of Miocene to Holocene age; south of the range, between the Hernandez and Ranchito shotpoints, the profile crosses similar sediments of Pliocene to Holocene age (Jennings and Strand, 1958).

Since 1979, additional seismic refraction data have been collected by the USGS near the Diablo Range profile in the Livermore Valley and near the Gabilan Range profile in the Salinas Valley. The more recent profiles are generally less than 50 km

long and thus define the velocities for the upper 10 km or less of the crust in these local areas. The deep crustal velocity structure of the Coast Ranges is inferred from our interpretation of 1967 data.

Unfortunately none of the refraction surveys provide information on the shear-wave velocity structure. However, Byerly (1939), Hamilton *et al.* (1964), Filson (1970), Boore and Hill (1973), Healy and Peake (1975), and Levander and Kovach (1981) have each made estimates of the shear-wave velocity for a single layer crust near or in the Gabilan and Diablo ranges by fitting least-squares to time-distance plots of earthquake or blast shear-wave arrivals that were recorded at local earthquake monitoring stations (Table 1). These least-square estimates do not resolve the details of the shear-wave velocity structure because the travel-time curves are sparsely sampled, and the earthquake source-to-station paths are not colinear. Without a detailed shear-wave velocity model to supplement the compressional-wave model, the geologic composition of the crust cannot be determined with certainty.

TABLE 1

ESTIMATES OF AVERAGE CRUSTAL SHEAR-WAVE VELOCITY IN CENTRAL CALIFORNIA (MANTLE VELOCITIES IN PARENTHESES)

Investigator	Geologic Terrane			Energy Source*
	Gabilan Range (km/sec)	San Andreas fault (km/sec)	Diablo Range (km/sec)	
Byerly (1939)	3.6	—	3.6	E
Hamilton *et al.* (1964)	3.4	2.9	—	B
Filson (1970)	—	3.0	3.6 (4.5 *Sn*)	E
Boore and Hill (1973)	3.5	2.8	—	E
Healy and Peake (1975)	3.5	2.9	—	E
Levander and Kovach (1981)	—	—	3.3 (4.35 *Sn*)	E

* E, earthquake; B, blast.

REINTERPRETATION OF THE DATA

Both the Diablo and Gabilan Range refraction profiles had five shotpoints spread along a profile line that extended approximately 200 km. Truck spreads 2.5 km long (Warrick *et al.*, 1961) were used in the interior parts of the profile. The recording station density for both profiles was greatest between the three innermost shotpoints, which were in the outcropping basement of the ranges (Figure 1). Beyond the interior shotpoints, station coverage was sparse. A catalog of the shotpoint and station data as well as plots of reduced travel-time record sections, is available in Warren (1978). Stewart (1968) made the preliminary interpretation of the first arrival travel-time data.

For this reinterpretation, the dipping-layer slope-intercept method was applied to the record section data (Figures 3 and 6) to derive the starting model. In the correlation of the refracted phases, particular care was taken to satisfy the required reciprocity of travel times along a given refractor between reversing shotpoints and to fit the refracted branch through the observed critical point on the record section. The velocity model was then refined using a two-dimensional ray-tracing program (Červený *et al.*, 1977). The starting model was input to the program in two arrays: one of 11 vertical grid lines spaced at 20-km intervals, in which the depths of the

layer boundaries were specified, and a second that specified the velocities above and below these grid lines. The program linearly interpolated both the boundary depths and the velocities between the defined grid lines. For a given model, groups of rays were projected from each shotpoint at takeoff angles ranging from nearly horizontal to vertical, thus producing a complete travel-time curve of refracted and reflected waves; subcritical and postcritical reflections were modeled as necessary. The velocity model was modified iteratively to produce better agreement between the calculated travel-time curves and the arrivals observed on the record sections. The calculated travel time for a ray was considered to be in good agreement with the observed travel time whenever the difference was less than 0.1 sec, although closer agreement was consistently sought. We assumed horizontal layers of uniform velocity in regions where the data does not provide constraints.

The Diablo Range models. Two alternative velocity models (Figure 2) were obtained from the analysis of the data (Figure 3, a through e). Model 1 is the preferred model, and model 2 is shown in part to illustrate the difficulties in uniquely fitting the sparsely observed arrivals from the lower crustal layers to a single model.

Above the basement, the poorly consolidated sediments in both models thin as the profile line leaves the Livermore Valley and enters the Diablo Range. The near-surface sediments of the Livermore Valley have velocities less than 3.0 km/sec (layer 1), and the underlying sediments (layer 2) have an average velocity of 4.2 km/sec. The depth to the top of the basement (layer 3) decreases from 3.4 km north of Livermore Valley to less than 0.2 km south of Livermore Valley. In model 1, the Franciscan basement consists of two layers. The upper layer (layer 3) is about 3 km thick and has top and bottom velocities of 4.8 and 5.2 km/sec. The lower layer (layer 4) extends to a boundary with the lower crust (layer 5) at 14.5 ± 0.5 km depth and has top and bottom velocities of 5.5 to 5.7 km/sec and 5.9 km/sec. In model 2, layers 3 and 4 have essentially the same average velocities as the two layers of model 1, but they have reduced thicknesses of 2 and 5 km, respectively. In model 2, the top of an additional mid-crustal layer (layer 4′) lies at 8 ± 1 km depth where its velocity is 6.0 km/sec. Layer 4′ is in contact with the lower crust (layer 5) at a depth of 18 ± 1 km. Along this lower boundary, the velocity in layer 4′ varies from 6.4 km/sec at the extremities of the model to 6.2 km/sec in the section between Mt. Stakes and Pacheco Pass.

In model 1, the velocities assigned at the top and bottom of the lower crust (layer 5) are 6.7 and 7.1 km/sec. In model 2, the velocities in layer 5 are the same as those of model 1 outside the Mt. Stakes-Pacheco Pass section, but within this section the top and bottom velocities are lower, 6.4 and 6.8 km/sec, respectively. In both models, the depth to Moho (boundary between layers 5 and 6) increases to the southeast: in model 1 from 28 ± 1 km near Benicia to 29 ± 1 km near Panoche Valley and in model 2 from 26 ± 1 to 29 ± 1 km. The 7.9 km/sec *Pn* velocity shown for both models (layer 6) was taken from a time-term analysis of regional earthquake arrivals (Eaton and Mooney, 1979) because clear *Pn* arrivals are lacking on the record sections. The crustal composition that can be inferred from these models is discussed in a later section.

Comparison of ray-trace models and observed data. To illustrate the comparative fit of these two models to the observed data, we have superimposed the travel-time curves, calculated by the ray-tracing program, for both models on each of the respective record sections of the Diablo Range profile (Figure 3, a through e). The branches of the travel-time curves are labeled using the letter and number code corresponding to the layers and boundaries shown in Figure 2.

As can be seen on the Benicia section (Figure 3a), the Cedar Mountain section (Figure 3b), and the Mt. Stakes section (Figure 3c), both models predict reasonably well the observed travel-time delays on branches $P3$ and $P4$, delays due to the dip of the basement to the northwest under the sediments of the Livermore Valley. On

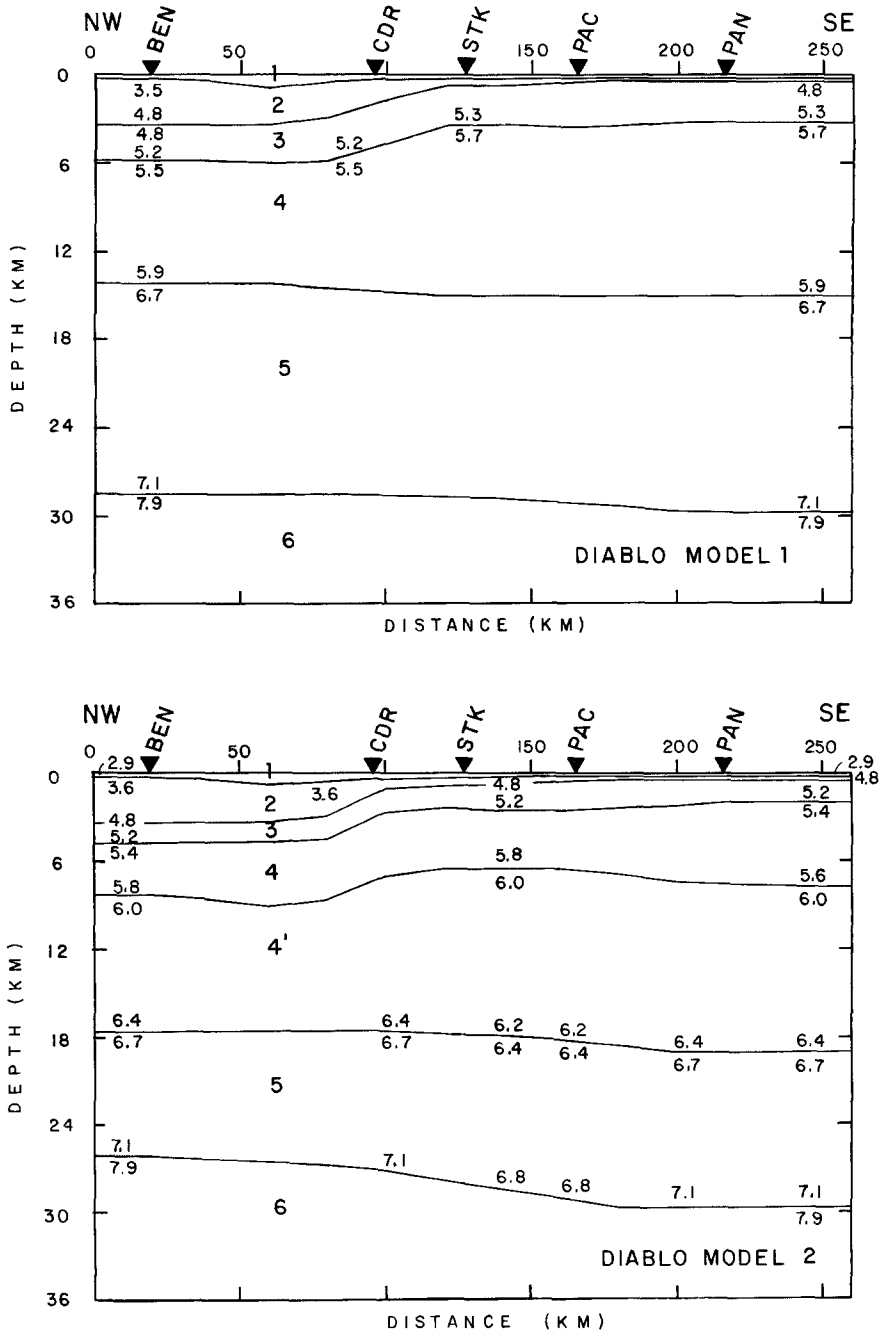

FIG. 2. Alternative two-dimensional velocity models derived for the Diablo Range profile by iterative ray tracing. Model 1 is the preferred model. For both models, the layers numbered consecutively from *top* to *bottom* are sediments (layers 1 and 2), Franciscan basement (layers 3, 4, and 4'), lower mafic crust (layer 5), and mantle (layer 6). The respective velocities assigned above and below the layer boundaries are labeled on each model. The relative positions of the shotpoints are shown by the labeled inverted triangles (see Figure 3, a to e, for abbreviations).

the Cedar Mountain and Mt. Stakes sections (Figure 3, b and c), the effect of these sediments is to produce a lower apparent velocity for the arrivals refracted to the northwest in the 5.5 to 5.9 km/sec layer (*P*4). To illustrate the travel-time delay encountered crossing the Livermore Valley, the travel-time curve for basement arrival southeast from Cedar Mountain are shown as a dotted line on the Cedar Mountain northwest section (Figure 3b).

The larger amplitude arrivals observed on both the Cedar Mountain and Mt. Stakes sections at ranges between 15 and 25 km southeast are predicted by both models 1 and 2 as being due to the reflection (*P*3*P*) from the top of the Franciscan assemblage, which forms the basement. On the same sections at ranges between 25 and 80 km southeast, the 5.7 km/sec (*P*4) branch predicted by model 1 agrees better with the observed arrival times and amplitudes than does the additional triplication (*P*4*P*′) and faster 6.2 km/sec branch (*P*4′) predicted by model 2. Other secondary arrivals seen on the Cedar Mountain section at ranges between 52 and 62 km southeast could be evidence for the reflection (*P*4*P*) from the upper crust-lower crust boundary as predicted by model 1. Precritical *PmP* arrivals (mantle reflection) seen at ranges between 38 and 75 km southeast on the Cedar Mountain section (Figure 3b), as well as at 63 km northwest and 42 and 62 km southeast on Mt. Stakes section, are scattered within 0.25 sec of the *PmP* (*P*5*P*) arrivals predicted by either model.

The best evidence for the high velocity in the lower crust is provided by the apparent velocity of the *PmP* branch (*P*5*P*) observed at ranges between 135 and 150 km southeast of the Benicia shotpoint (Figure 3a). These observed *PmP* arrivals move forward in time and approach the predicted 6.9 km/sec branch (*P*5). However, the *PmP* arrivals observed in the reversing direction on the Panoche Valley section (Figure 3e) at ranges greater than 65 km northwest are uniformly later than those predicted by either model, later by as much as 0.5 sec. If this delay of the *PmP* arrivals between Mt. Stakes and Panoche Valley (Figure 3, c through e) can be attributed to the lower crust, then the average travel time in the lower crust needs to be increased, either by decreasing the lower crustal velocities or by thickening the lower crust toward the southeast. However, we were not able to make a simple change in our models that would improve the agreement with the observed *PmP* arrivals for the Panoche Valley section without also causing disagreements with the observed *PmP* arrivals for the Benicia and Cedar Mountain sections (Figure 3, a and b).

Blümling and Prodehl (1982) interpreted this arrival not as *PmP*, but as a reflection from the bottom of a lower crustal, low-velocity zone (LVZ). To test their LVZ velocity model (described below), they measured the true amplitudes of the reflection observed on the Cedar Mountain section at ranges between 40 and 135 km southeast and then compared them with computed synthetic seismograms for various models (Fuchs and Müller, 1971). Their comparison of the observed and synthetic seismograms showed amplitude maxima at the correct distances for their LVZ model, but the amplitude ratios between phases are incorrect. They attributed the dissimilarity of the amplitude ratios to lateral heterogeneity in the velocity structure.

Comparison with previous studies. Byerly (1939) studied the velocity structure of the central Coast Ranges east of the San Andreas fault. He used the arrivals from 17 earthquakes that were recorded by five seismograph stations operated by the University of California at Berkeley. His crustal model consists of two layers that have velocities of 5.61 and 6.72 km/sec and thicknesses of 9 and 23 km, respectively, for a total crustal thickness of 32 km. Tocher (1955), using the same array of stations

as Byerly (1939) but including more earthquakes and a quarry blast, derived a model similar to Byerly's; the major difference was that the lower crust in Tocher's model has a velocity of 6.5 km/sec.

Stewart (1968) analyzed the seismic refraction data that we have reinterpreted.

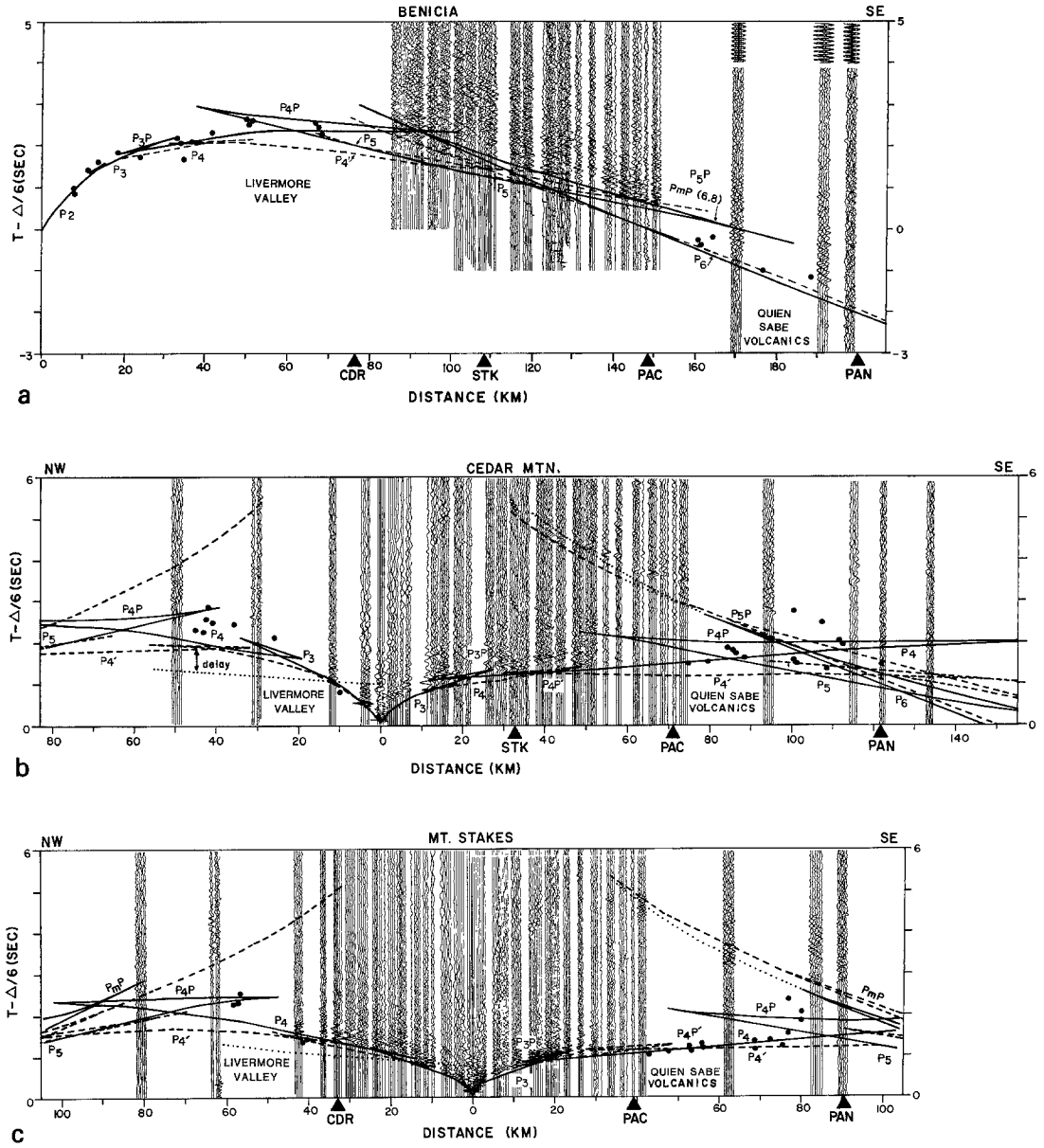

FIG. 3. Record sections for the Diablo Range profile: (a) Benicia (BEN); (b) Cedar Mountain (CDR); (c) Mt. Stakes (STK); (d) Pacheco Pass (PAC); and (e) Panoche Valley (PAN). The data plotted in each section consist of seismograms taken from truck spreads and arrival-time picks (solid dots) taken from portable tape-recording seismographs. The solid travel-time curves are those obtained by two-dimensional ray tracing of model 1 (Figure 2); the dashed travel-time curves are from model 2 (Figure 2). Selected branches of these travel-time curves have been labeled according to the following convention: diving rays that bottomed in a given layer N are labeled P_n, where n corresponds to the layer number assigned in Figure 2; the rays that reflected from a given boundary n are labeled P_nP. The reflection from the base of the crust, P_5P, is labeled P_mP. On each section, the locations of the other shotpoints are indicated by solid triangles. In addition, the relative locations of the Livermore Valley and the Quien Sabe Volcanics are labeled. The time separation between the travel-time curves and the dotted lines shows the time delay caused by the thicker sedimentary section in the Livermore Valley.

His model for the Diablo Range (Figure 4) has layers that have velocities of 3.4, 5.0, 5.6, and 6.9 km/sec and respective thicknesses of 1, 2, 10, and 18 km, for a total crustal thickness of 31 km. The 3.4 km/sec layer increases in thickness from 1 to 4 km as it leaves the range and enters the Livermore Valley from the south. Stewart placed the bottom of the Franciscan assemblage (5.6 km/sec) at a depth of 13 ± 3 km in comparison to our estimates of 16 ± 3 km.

Healy and Peake (1975) derived an upper crustal velocity model for the Diablo Range from a composite of Stewart's travel-time data and additional earthquake travel-time data, which was recorded by seismic stations straddling the San Andreas fault southwest of the Pacheco Pass shotpoint (Figure 1). Their model consists of four layers that have velocities of 4.9, 5.4, 5.7, and 6.8 km/sec and respective

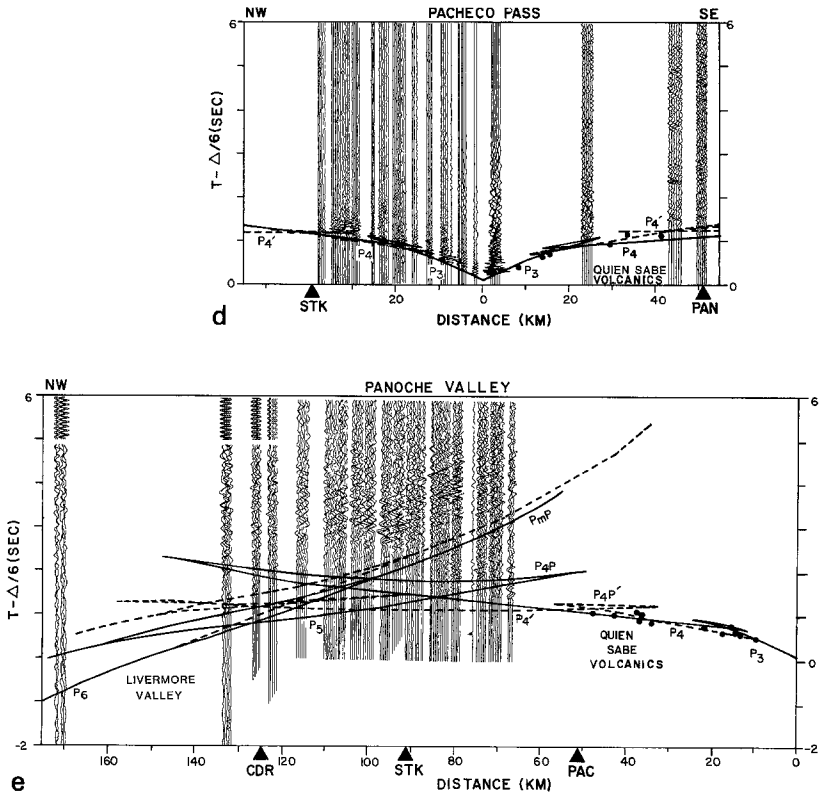

FIG. 3. Continued.

thicknesses of 3.0, 4.5, and 3.5 km, for a total depth of 11 km to the 6.8 km/sec layer; they did not determine the thickness of the 6.8 km/sec layer.

Steppe and Crosson (1978) derived a model using a least-squares inversion method applied to local earthquake data recorded near the San Andreas and Calaveras faults south of Pacheco Pass. In their model, the velocity increases continuously and the velocity gradient decreases stepwise as depth increases (Figure 4). The velocity of 6.0 km/sec occurs at a depth of 6 km in their model.

Blümling and Prodehl (1982) used procedures analogous to ours to develop a velocity model for the Diablo Range from the refraction profile data and local earthquake arrival-time from Prodehl (1977). In their velocity model, the upper 12 km of the crust has a velocity structure that is very similar to our model 1 (Figure

4). Below 12-km depth, the velocity in their model increases from 5.8 to 6.8 km/sec over 2.5-km depth; the 6.8 km/sec velocity extends to a depth of 21 to 22 km, where the average velocity decreases to 5.3 km/sec in a 4- to 5-km-thick LVZ. At 26-km depth, the LVZ is terminated by a discontinuous velocity increase to 7.6 km/sec; the 7.6 km/sec velocity extends to the crust-mantle boundary at a depth of 29 km.

Figure 4 shows the velocity-depth functions of our ray-trace models, taken at a point mid-way between Mt. Stakes and Pacheco Pass, compared with the velocity-depth functions derived by Stewart (1968), Steppe and Crosson (1978), and Blümling and Prodehl (1982). This comparison shows that the estimated thickness of the upper crust is between 13 km (Stewart, 1968) and 18 km (model 2, this study). Three of the models have the boundary at 14 ± 1 km depth above and below which the velocities are 5.8 ± 0.1 and 6.8 ± 0.1 km/sec, respectively. The continuous increase of velocity with depth in the model of Steppe and Crosson (1978) appears to have

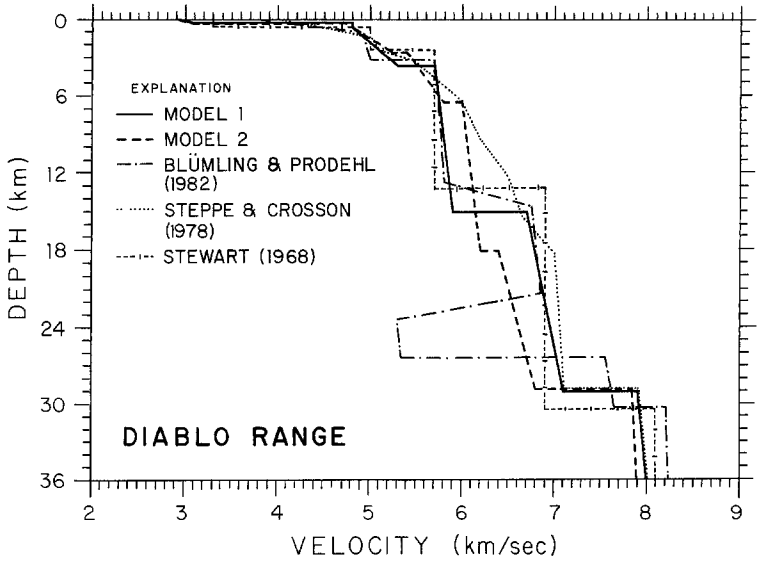

FIG. 4. The velocity-depth functions are plotted for both of the Diablo Range ray-trace models (Figure 2) taken at a point between Mt. Stakes and Pacheco Pass. Also plotted are the velocity-depth functions derived by Stewart (1968), Steppe and Crosson (1978), and Blümling and Prodehl (1982).

overestimated the velocity between 7- and 14-km depth. The lower crust in all the models except that of Blümling and Prodehl (1982) has velocities between 6.6 and 7.1 km/sec. As previously discussed, the model of Blümling and Prodehl (1982) shows a pronounced low-velocity layer (5.3 km/sec) between 22- and 26-km depth. We did not test a low-velocity model in our interpretation of the data; verification of the proposed LVZ requires the recording of more amplitude-controlled data in the Diablo Range.

Gabilan Range models. Figure 5 shows the two alternative velocity models we derived for the Gabilan Range profile. Except for the lower crustal structure, our two ray-trace models are almost identical. Model 1 is the preferred model; model 2 is presented to illustrate effect of a high-velocity (mafic) layer in the lower crust.

Both models show the Gabilan Range flanked by sedimentary aprons about 2 km thick; the younger sediments southeast of the range have lower velocities (2.4 km/sec at the top and 3.8 km/sec at the bottom) than the older, more consolidated sediments northwest of the range (3.6 to 4.6 km/sec). In both models, the uppermost

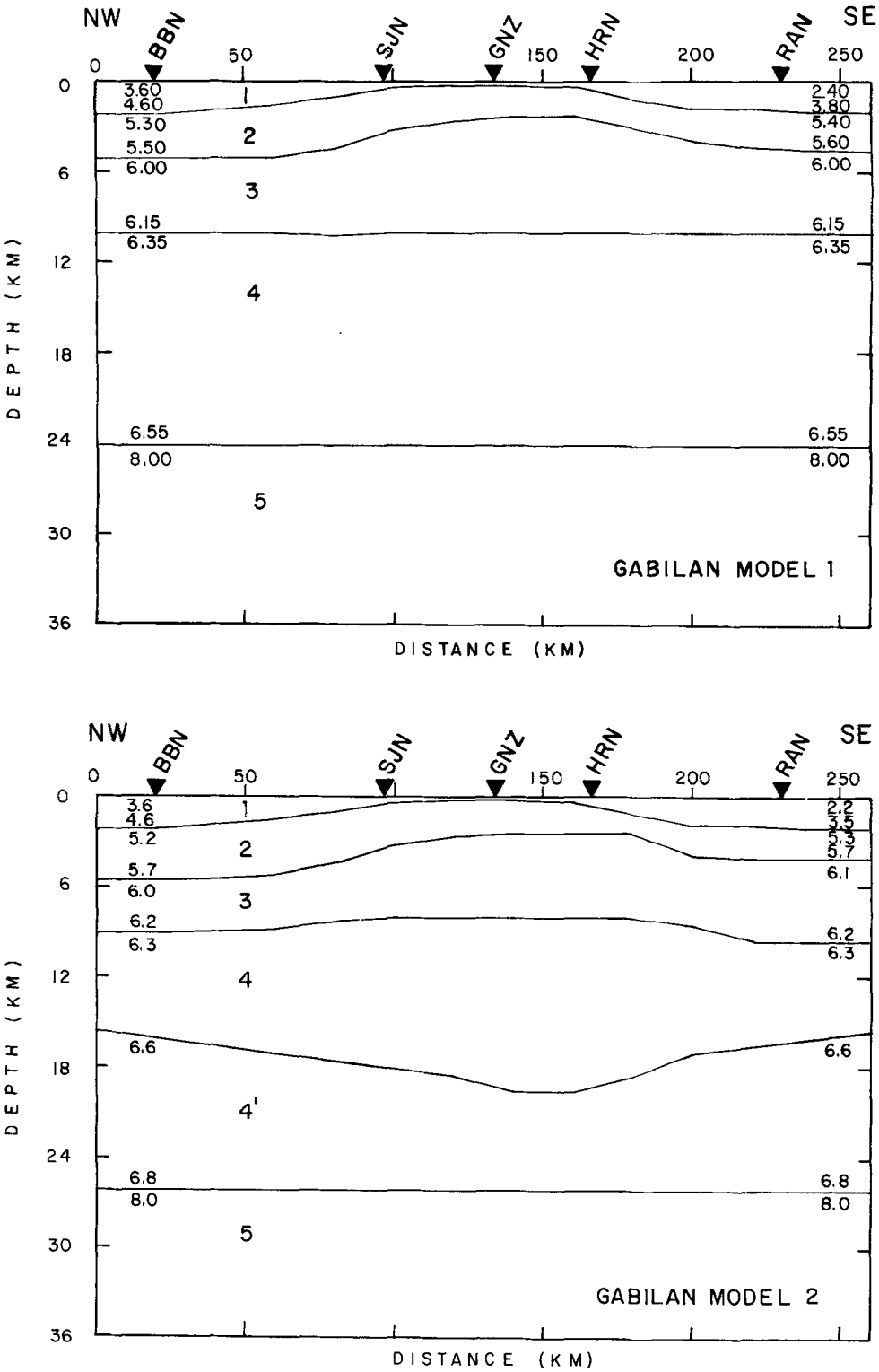

FIG. 5. Models 1 and 2 show alternate two-dimensional models derived for the Gabilan Range profile by iterative ray tracing. Layers numbered consecutively from *top* to *bottom* represent sediments (layer 1), upper granitic basement (layers 2 and 3), lower basement (layers 4 and 4'), and mantle (layer 5). The velocities assigned above and below the layer boundaries are labeled. The relative positions of the shotpoints are indicated by the inverted triangles (see Figure 6, a to e, for abbreviations).

basement layer (layer 2) has an average velocity of about 5.45 km/sec, shallows to a depth near zero beneath the range, and is between 2 and 3 km thick. Layer 3 has an average velocity of 6.1 km/sec (6.0 to 6.2 km/sec); the boundary between layers 2 and 3 shallows from 5.5-km depth under the valleys to 2.3 km under the range.

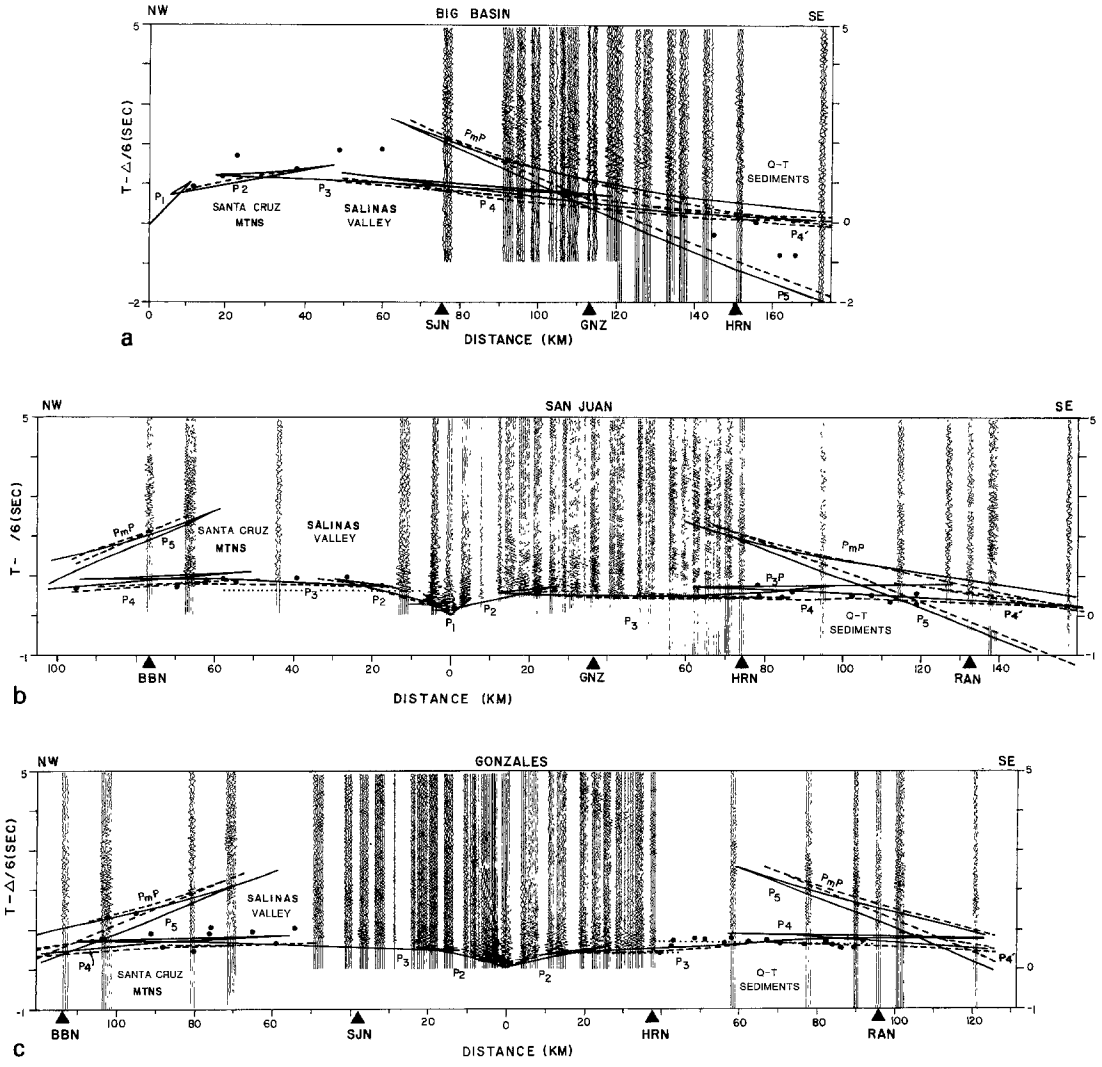

FIG. 6. Record sections for the Gabilan Range profile: (a) Big Basin (BBN); (b) San Juan (SJN); (c) Gonzales (GNZ); (d) Hernandez (HRN); and (e) Ranchito (RAN). The data plotted on each section consist of seismograms from truck spreads and arrival-time picks (solid dots) taken from portable tape-recording seismographs. The solid travel-time curves are those obtained by two-dimensional ray tracing of model 1 (Figure 5); the dashed travel-time curves are from model 2 (Figure 5). Branches of these travel-time curves have been labeled using the convention described for the Diablo Range sections in Figure 3. The time separation between the travel-time curves and the dotted lines is the time delay caused by thicker sediments south of the range. The locations of the other shotpoints are indicated (solid triangles). Also labeled are the relative locations of the Santa Cruz Mountains, the Salinas Valley, and the Tertiary and Quaternary sedimentary deposits (Q-T, south of the range).

The two models differ in velocity structure beneath layer 3. In model 1, the top of layer 4 has a velocity of 6.35 km/sec and is horizontal at a depth of 10 km; in model 2, the top of this layer bulges upward and is 1 or 2 km shallower. Model 1 has a one-layer lower crust (layer 4), and the base of the crust is assigned a velocity of 6.55 km/sec. Model 2 includes an additional lower crustal layer (layer 4′) that has an

average velocity of 6.7 km/sec (6.6 to 6.8 km/sec), similar to that found beneath the Diablo Range. The depth to the top of this layer increases from 16 km beneath the flanking valleys to 19 km beneath the range.

Because of the uncertainties in the lower crustal velocities, the calculated depth to the Moho is not well constrained. The Moho is horizontal at a depth of 24 km in model 1 and at 26 km in model 2. As was the case for the Diablo Range profile, the *Pn* velocities of 8.0 km/sec shown for the Gabilan Range models (layer 5) were taken from a time-term analysis of regional earthquake arrivals (Eaton and Mooney, 1979).

Comparison of ray-trace models and observed data. In Figure 6, a through e, we have superimposed the travel-time curves derived by two-dimensional ray-tracing, for the two crustal models (Figure 5), on the respective record sections of the Gabilan Range profile. We have used the same labeling convention as on the Diablo Range sections (Figure 3 a through e).

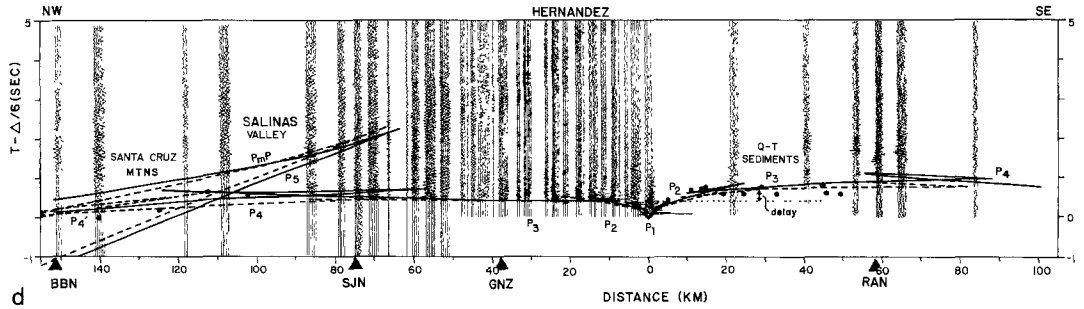

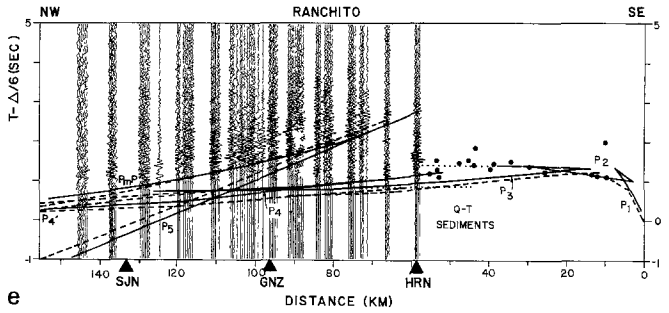

FIG. 6. Continued.

At distance ranges of less than 50 km, the travel-time curves (*P*1 to *P*3) predicted by ray-trace models are essentially identical and are in good agreement with the observed data. The dotted lines projected on the San Juan, Gonzales, Hernandez, and Ranchito sections (Figure 6 b through e) illustrate the time-delay offset of the 6.1 km/sec branch (*P*3) resulting from the overlying sedimentary cover. North of the Gabilan Range between Big Basin and San Juan, the delays attributable to the sediments are less than 0.2 sec, although south of the range between Hernandez and Ranchito, the delays are about 0.25 sec. On the Ranchito section, the first arrivals (*P*3) advance 0.4 sec as they cross the range north of Hernandez.

At distance ranges between 55 and 75 km southeast of the San Juan shotpoint (Figure 6b), possible reflections from the top of an intermediate-velocity layer (*P*3*P*) are seen about 1 sec behind the first arrivals near the *P*3*P* triplication cusp predicted by model 1. Other indications of either a locally faster basement or a structural rise in basement layers are the 6.3 km/sec apparent velocity branch observed between

43 and 68 km southeast of the San Juan shotpoint and the early first arrivals (0.2 sec) seen near the Santa Cruz Mountains 66 to 76 km northwest of the San Juan shotpoint (Figure 6b).

The presence or absence of a 6.7-km/sec or high-velocity, lower crustal layer in the Gabilan Range cannot be definitely established, due to the lack of clear *PmP* arrivals. At distance ranges greater than 125 km on the Big Basin section (Figure 6a), the *PmP* (*P4P*) branch moves forward but the arrival quality is not sufficient to establish whether the *P4P* branch predicted by model 1 or the *P4P'* branch predicted by model 2 best fits the data. In the reversing direction, the *PmP* arrivals seen on the Ranchito section (Figure 6e) at distance ranges greater than 60 km northwest approach a velocity slightly greater than 6 km/sec; they are better fit by model 1, which lacks the 6.7 km/sec layer in the lower crust in model 2.

Possible precritical *PmP* reflections are seen on the San Juan (47 to 55 km southeast), Gonzales (22 to 38 km southeast), and Hernandez (42 to 52 km northwest) sections (Figure 6, b through d) and have arrival times between 2.5 and 3.5 sec. The *P4P* arrivals predicted by model 1 are late by as much as 0.25 sec, but the *P4P'* predicted by model 2 are late by over 1 sec; possibly these reflections are from the top of a basal crustal layer just above the Moho. Secondary arrivals later than the predicted *PmP* are found on both the Gonzales section (71 km northwest) and the Hernandez section (107 and 140 km northwest); these arrivals may result from a discontinuous velocity structure below the Moho.

Comparison with previous studies. McEvilly (1966) and Chuaqui and McEvilly (1968) used a large array and numerous earthquakes and explosions to study the velocity structure near the San Andreas fault east of the Gabilan Range. In their 1968 model for the upper crust (0 to 7 km), the velocity follows the relation $v = 5.33 + 0.03\ Z$, where Z is the depth in kilometers. This relation yields a velocity of 5.54 km/sec at 7-km depth. Below 7 km their model follows the relation $v = 5.14 + 0.06\ Z$, which yields a velocity of 6.10 km/sec at 16-km depth and 6.34 km/sec at 20-km depth.

Stewart (1968) reported that the record sections along the Gabilan Range profile (Figure 6, a through e) were more difficult to interpret than those of the Diablo Range. Within the Gablian Range, he reported a 4.8 km/sec surface layer overlying a 6.1 km/sec basement. He did not develop a complete upper crustal model, but using his travel-time interpretation, we calculate a depth of about 1.5 km to basement. On the San Juan section southeast of the shotpoint, the 6.1 km/sec apparent velocity increases at the 38-km range to an apparent velocity of 6.3 km/sec. Coincident with this higher apparent velocity, he also reported that the seismic amplitudes for arrivals in the range 38 to 75 km decay as X^{-6}, where X is distance. He interpreted this attenuation as evidence for a LVZ at a depth no greater than 10 km. Although Stewart's observation of amplitude decay stands, our models have no LVZ because we found no persuasive evidence on the record sections of either time-offset reflection branches or distinctive shadow zones. (We discuss the question of a LVZ more thoroughly in a later section.)

Healy (1963) and Prodehl (1979) studied a 250-km-long profile between shotpoints at San Francisco, Camp Roberts, and Santa Monica Bay, southern California. This profile was recorded approximately parallel to the Gabilan Range profile, but it is 15 km closer to the coast. Because the basement along this profile consists largely of the same plutonic rocks as those that make up the Gabilan Range (Ross, 1978), it is useful to compare their interpretations of crustal structure to that presented here. The crustal model of Healy (1963) consists of two layers that have velocities of 3.0

and 6.1 km/sec and respective thickness of 1 and 21 km; he also discussed the possibility that a lower crustal layer having a higher velocity was undetected by the profiles. Prodehl (1979) proposed a model that has a rapid velocity increase from 4.5 to 6.0 km/sec in the upper 9 km and a gradual velocity increase from 6.0 to 6.4–6.5 km/sec at the crust-mantle boundary at 26-km depth. Thus, the model of Prodehl (1979) is consistent with the suggestion of Healy (1963) that the lower crust might have a velocity greater than 6.1 km/sec.

Hamilton *et al.* (1964) studied another profile that was recorded in the Salinian block and had shotpoints near San Francisco and Salinas. They interpreted the crustal structure to consist of a surface layer having a velocity of 4.16 km/sec and a thickness of 1 to 3 km overlying a layer having a velocity of 6.2 km/sec and a thickness of 19 to 21 km, thus giving a total crustal thickness of 20 to 24 km.

Healy and Peake (1975) studied the southern Gabilan Range using earthquake recordings from a local seismograph array located near the San Andreas fault. Their

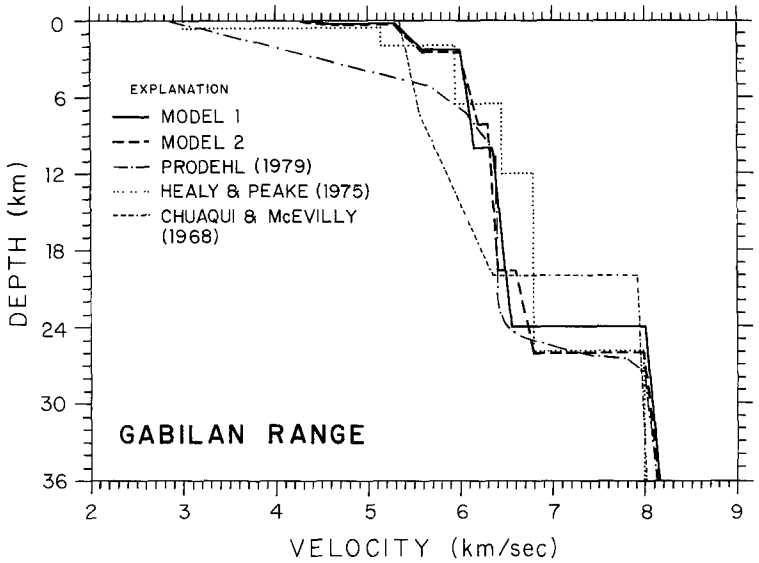

FIG. 7. The velocity-depth functions for both of the Gabilan Range ray-trace models (Figure 5) at a point near Gonzales are plotted along with the velocity-depth functions derived by Chuaqui and McEvilly (1968), Healy and Peake (1975), and Prodehl (1979).

study is the only one to report clear evidence for a 6.8 km/sec layer in the crust of the Gabilan Range. Their crustal model consists of four layers that have velocities of 5.15, 5.95, 6.45, and 6.8 km/sec, the upper three layers having respective thicknesses of 1.5, 4.5, and 5.5 km for a total depth of 11.5 km to the top of the 6.8 km/sec layer; the Moho is at 28-km depth. To compare the theoretical travel-time curves produced by their model and the seismic refraction data, we traced rays through their model. We found that placing the 6.8 km/sec lower crustal layer at a depth of 11.5 km and the Moho is at 28-km depth results in predicted *PmP* arrivals that are increasingly early at distance ranges greater than 100 km, because the average crustal velocity along the travel path is at least 0.25 km/sec too high. The 6.8 km/sec layer is therefore not as shallow as 11.5 km on a regional scale in the Gabilan Range.

Figure 7 compares the velocity-depth functions of the ray-trace models at a point joint south of the Gonzales shotpoint with the velocity-depth functions derived by

Chuquai and McEvilly (1968), Healy and Peake (1975), and Prodehl (1979) for the Gabilan Range. The model of Chuaqui and McEvilly (1968) has lower velocities than the other models throughout the crust possibly because the model is for the crust near the San Andreas fault which is highly fractured. The model of Prodehl (1979) is similar to our model 1 except that it has lower velocities above 6-km depth and a 2 km thicker crust. Both models indicate a 6.4 km/sec velocity below 10-km depth in disagreement with the 6.8 km/sec velocity of Healy and Peake (1975). In summary, our models 1 and 2 appear to adequately represent the range of possible velocity-depth models for the Gabilan Range.

Crustal Composition of the Diablo and Gabilan Ranges

Seismic velocity structure may be used to infer crustal composition because velocity-rock-type relationships have been determined by laboratory measurements of both compressional- and shear-wave velocities in rocks at elevated pressures and temperatures. When both velocities are known for a part of the crust, its possible composition can be rather narrowly restricted (Christensen and Fountain, 1975). In this report, we have determined only the compressional-wave velocity structure and the available information on the shear-wave structure (Table 1) generally consists of an average velocity for the entire crust, as compared to our more detailed compressional-wave structure. Thus, we are unable to take complete advantage of the laboratory velocity-composition relationships. One constraint provided by the combined velocity information that is satisfied by the rock compositions discussed below is that Poisson's ratio in the crust be in the range of 0.24 to 0.27. In the discussion that follows, we rely heavily on geologic inference in constructing compositional models. We will argue that some models are more plausible than others, on the basis of the surface geology and the compressional-wave velocity structure.

Lin and Wang (1980) have discussed the composition of the crust of both the Diablo and Gabilan ranges, and Stewart and Peselnick (1977, 1978) discussed the crustal composition of the Diablo Range. Figures 8 and 9 compare our velocity-depth functions with their measurements of rock velocities at elevated pressures and temperatures. Figure 10 compares our functions to new laboratory measurements presented by Kern and Richter (1981).

TABLE 2

Geothermal Temperature Estimates

Depth (km)	$T1$*	$T2$†	$T3$‡	$T4$§
0	20	20	20	20
5	90	150	170	200
10	160	270	310	360
15	220	350	450	470
20	290	415	580	585
25	360	480	715	700
30	430	545	850	815
	⟵COLD ⟶		⟵ HOT ⟶	

* Cold Precambrian crust (Theilen and Meissner, 1979).

† "Cold" estimate of California crust (Lachenbruch and Sass, 1973).

‡ "Hot" estimate of California crust (Lachenbruch and Sass, 1973).

§ "Hot" continental crust (Theilen and Meissner, 1979).

A comparison of laboratory and field measurements requires an estimate of the temperature in the crust at depth. Four such estimates for continental crust are shown in Table 2. Geotherm $T1$, presented for reference, shows that in cold Precambrian crust [1.1 heat flow units (HFU)], the temperature increases from 20°C at the surface to ~430°C at 30-km depth (Theilen and Meissner, 1979). Geotherms $T2$ and $T3$ are estimates for the Coast Ranges (2.0 HFU) that Lachenbruch and Sass (1973) derived using different assumptions about the distribution of

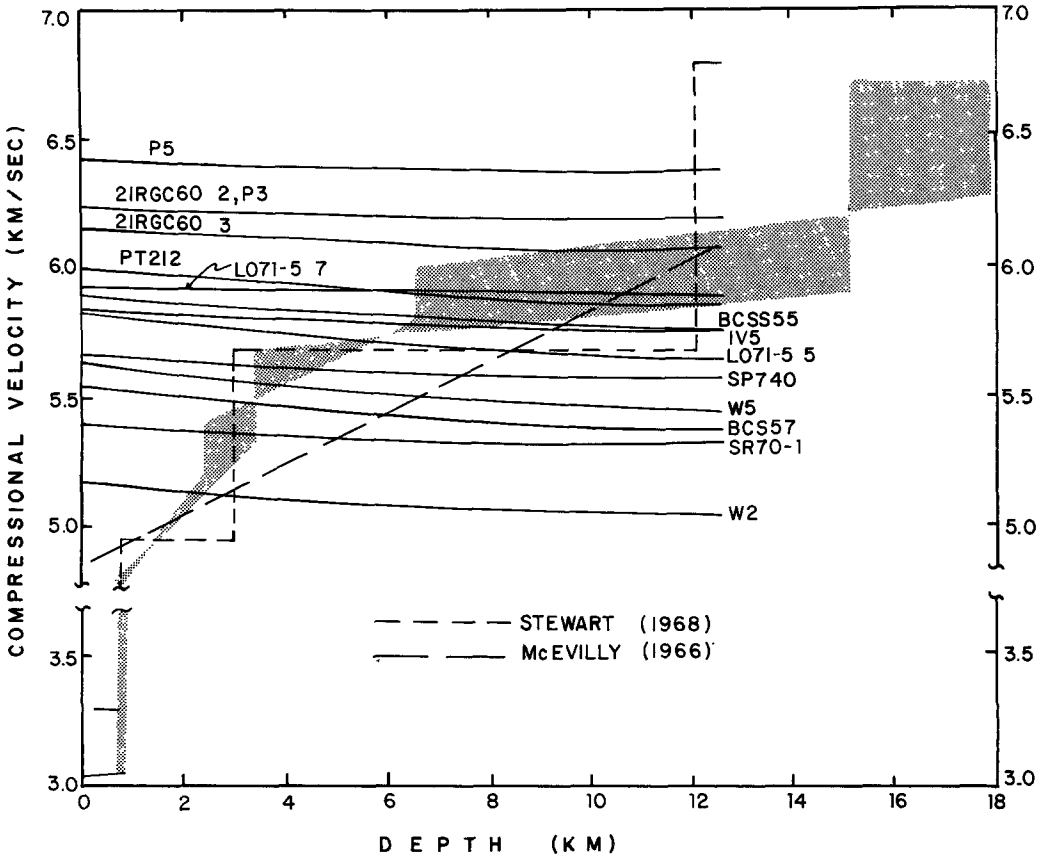

FIG. 8. Velocity-depth functions calculated from laboratory measurements of Franciscan rocks (Stewart and Peselnick, 1978) are compared to a composite velocity-depth function for the Diablo Range derived from ray-trace models shown in Figure 2. The outer bounds of the *shaded* velocity-depth function are the actual calculated functions for models 1 and 2. The *shaded area* shows the range of possible models, but it does not constitute a formal velocity bound in a mathematical sense. Curves are labeled for rock samples of Stewart and Peselnick (1978): W2 and W5 are graywackes; SR70-1 and SP740 are slightly recrystallized graywackes; BCS57 is slightly recrystallized shale; IV5 is recrystallized graywacke; L071- (5 and 7) are pumpellyite-bearing sandstones; BCSS55 is pumpellyite prehnite-bearing graywacke; PT212 is lawsonite-bearing melange matrix; and 21RGC60- (2 and 3), P3 and P5 are jadeite metagraywackes.

crust and mantle heat sources. Geotherm $T4$ is an additional estimate for continental crust that has a heat flow of 2.0 HFU (Theilen and Meissner, 1979). Note that estimates $T3$ and $T4$ are in close agreement.

In this discussion, we use geotherm $T2$ for the "cold" estimate of Coast Range crustal temperature and geotherms $T3$ and $T4$ interchangeably for the "hot" estimate. The cold and hot estimates differ by ~110°C at a depth of 15 km. Because laboratory measurements (e.g., Stewart and Peselnick, 1978; Christensen, 1979; Lin

and Wang, 1980; Kern and Richter, 1981) show that for most rocks a temperature increase of 110°C results in a velocity decrease of 0.04 km/sec or less, the velocity-depth profile in the upper 15 km of crust is largely independent of the geothermal gradient. However, the calculated velocity-depth profile in the lower crust is more sensitive to the assumed geothermal gradient for two reasons: first, the temperature estimates for cold and hot crusts differ by as much as 305°C at 30-km depth (545°C versus 850°C), and second, nonlinear velocity-temperature effects at temperatures above ~400°C (Christensen, 1979) may cause a dramatic velocity decrease. Therefore, inferences of crustal composition for the lower crust are less certain than for the upper crust.

Diablo Range. We will not discuss the Tertiary and Quaternary sediments overlying the basement, because their velocity-depth structure is not well determined by this refraction data. Available geologic surface mapping and drill-hole data better determine the near-surface composition.

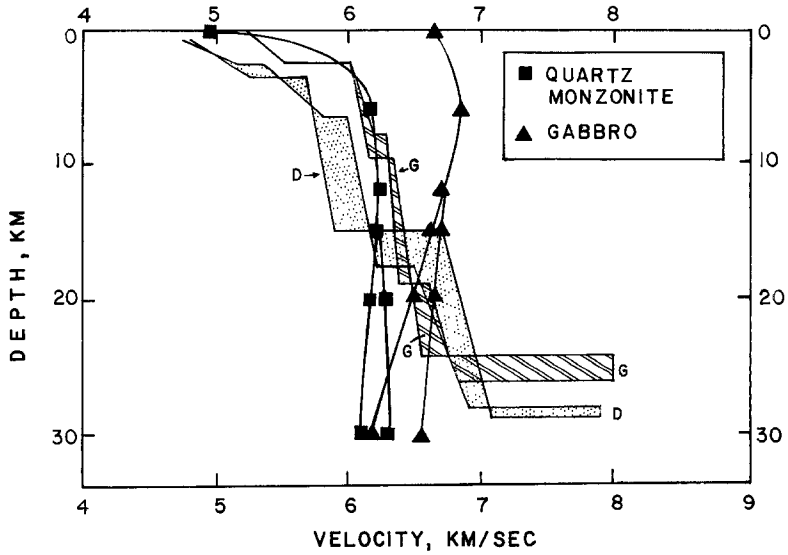

FIG. 9. Velocity-depth functions calculated from laboratory measurements of quartz monzonite and olivine-hornblende gabbro (Lin and Wang, 1980) compared to the composite velocity-depth functions derived by our ray-trace modeling of the Diablo (D) and Gabilan ranges (G).

As discussed earlier, the Franciscan assemblage is the major component of the basement in the Diablo Range. According to Bailey *et al.* (1964), approximately 90 per cent of the Franciscan assemblage consists of a melange composed mainly of graywacke, sandstone, cherts, and shales; the remaining 10 per cent consists of volcanic rocks, mainly metabasalts. Within the sedimentary units, minerals such as jadeitic pyroxene, pumpellyite, lawsonite, and glaucophane are present, indicating that these rocks have been subjected to a high-pressure, low-temperature metamorphism (Bailey *et al.*, 1964; Ernst, 1965).

Our interpretation of the refraction data indicates the upper crust has a thickness of 16 ± 3 km and is underlain by a higher velocity lower crust. Estimates of lithostatic pressure for a given depth can be calculated using: $P(\text{Gpa}) = Z*D/100$, where P is pressure in giga-Pascals, Z is the depth in kilometers, and D is an average density of 2.8 gm/cm^3. Thus, within the upper crust the lithostatic pressure increases from 0 to 0.45 ± 0.09 Gpa. The temperature increases from 20°C to about 320° to 470°C (geotherms $T2$, $T3$, Table 2).

Both Stewart and Peselnick (1977, 1978) and Lin and Wang (1980) have made laboratory measurements of the velocity of Franciscan metasedimentary deposits and volcanic rocks at these pressures and at temperatures up to 350°C. Figure 8 shows the experimental results of Stewart and Peselnick (1978) plotted with the velocity-depth functions determined by our ray-trace models for the upper crust of the Diablo Range. This comparison shows that our velocity-depth functions are well within the range of velocities measured for graywackes and metagraywackes and they tend to be most similar to the velocity of metagraywacke at depths greater than 6 km. We, therefore, agree with Stewart and Peselnick (1980) and Lin and

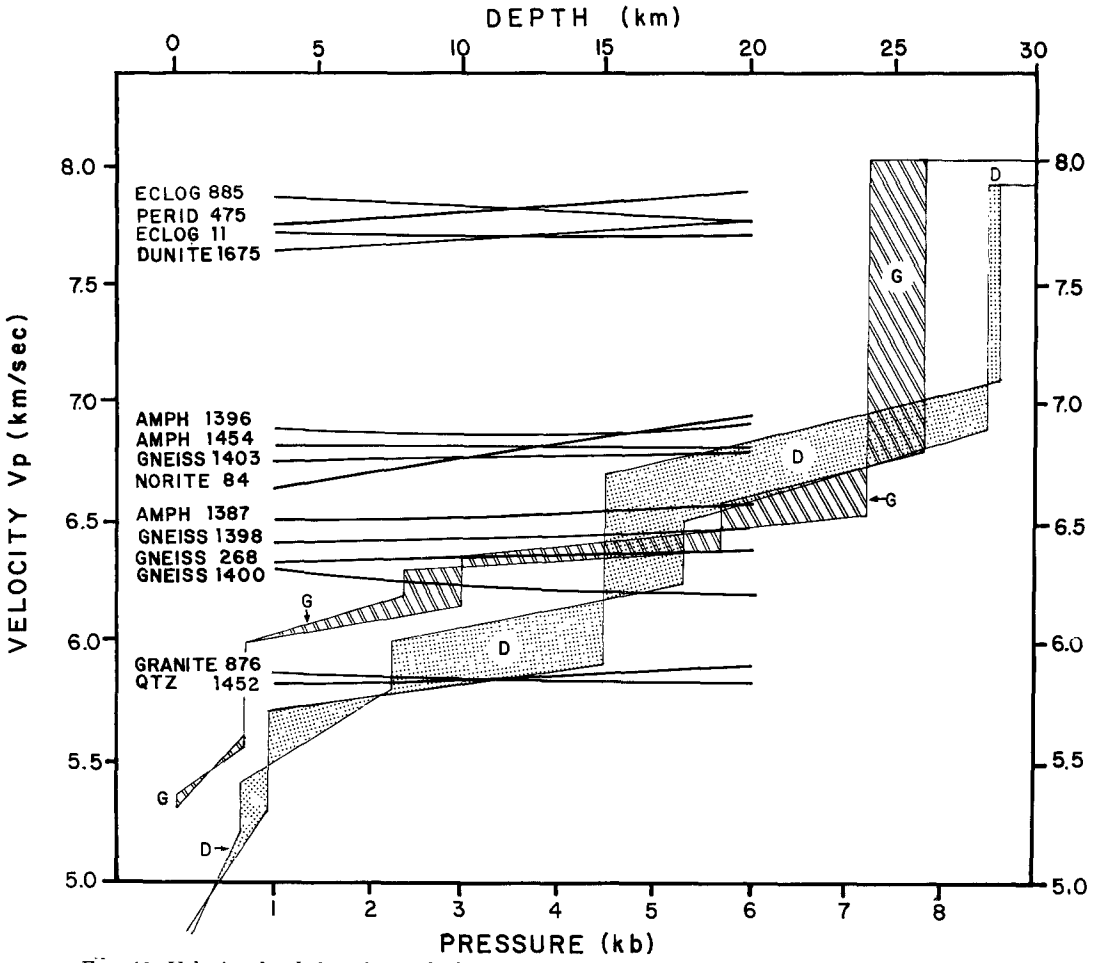

FIG. 10. Velocity-depth functions calculated from laboratory measurements of 15 rock samples which show a wide range of mineralogical and chemical compositions (Kern and Richter, 1981) compared to our composite velocity-depth function for the Diablo (D) and Gabilan ranges (G). Abbreviations: eclog, eclogite; perid, peridotite; amph, amphibolite; qtz, quartzite.

Wang (1980) that the 16-km-thick upper crust of the Diablo Range consists of Franciscan rocks.

We next turn to the question of the composition of the lower crust in the Diablo Range. Our ray-trace models for the crust show that the velocity increases discontinuously at 16 ± 3 km depth from 5.9 to 6.2 to 6.4 to 6.7 km/sec, followed by a velocity gradient of +0.03 km/sec/km down to the crust-mantle boundary at a depth of 28 ± 2 km. At the depths in question, the lithostatic pressure increases from about 0.45 to 0.78 Gpa, and the temperature increases from about 360° to

495°C to about 520° to 795°C (Table 2). Measurements of rock velocities at these pressures and temperatures are provided by Lin and Wang (1980) and Kern and Richter (1981).

Lin and Wang (1980) measured velocities at up to 0.7 Gpa and 450°C in both quartz monzonite and olivine-hornblende gabbro, and they used the two geotherms of Lachenbruch and Sass (1973; $T2$ and $T3$ in Table 2) to calculate velocity-depth functions for these two rock types. When we compare Lin and Wang's functions to those derived from our velocity models (Figure 9), we see that the modeled velocity for the lower crust of the Diablo Range is significantly higher at all depths than the velocity of the quartz monzonite sample. The modeled velocity is, in fact, in agreement with the velocity of the gabbro samples at 16- to 20-km depth, although it is 0.4 to 0.9 km/sec higher than the velocity of gabbro at 27-km depth. We further note that the laboratory data indicate that the velocity-depth function for quartz monzonite and gabbro will have a negative velocity gradient in the lower crust, due to temperature effects. A possible explanation of the positive velocity gradient in our velocity-depth function is a gradual compositional change toward denser crustal minerals as depth increases.

Kern and Richter (1981) measured velocities in a variety of rock types at up to 0.6 Gpa and 700°C, and they used geothermal gradient $T4$ (Table 2) to calculate the expected velocity-depth functions (Figure 10). Linear extrapolations of the laboratory velocity-depth functions for samples of amphibolite, gneiss, and norite agree well with that modeled for the lower crust of the Diablo Range, although we note once again that, except for the norite sample, the laboratory functions do not show the positive velocity gradient of our modeled (refraction) function.

Stewart and Peselnick (1978) and Lin and Wang (1980) have already argued for a gabbroic composition for the lower crust in the Diablo Range. The data of Kern and Richter (1981) broaden the range of possible compositions to include amphibolite, gneiss, and norite. Because our velocity-depth functions for the lower crust provide evidence of a gradual change in composition as depth changes, one possible composition, which agrees with the laboratory data and geologic models supporting accretion of the Franciscan assemblage to the top of an oceanic plate, is a mixture of gabbro and amphibolite without any norite or gneiss.

Gabilan Range. We infer the compositon of the crust of the Gabilan Range using the same method as above. Unlike the Diablo Range, the Gabilan Range is difficult to simply divide into an upper and a lower crust. Our interpretation of the velocity structure indicates either a single small seismic discontinuity (0.2 km/sec) at 10 km (Figure 5, model 1) or two small discontinuities at 9 and 18 km (Figure 5, model 2). Because the surface of the Gabilan Range consists of granitic rocks, we compare the modeled velocity structure with laboratory velocity measurements of samples of quartz monzonite (Figure 9) or similar rocks (Figure 10). The quartz monzonite measurements (Figure 9) of Lin and Wang (1980) are in excellent agreement with the interpreted structure in the 0- to 9-km depth range; the granite measurements (Figure 10) of Kern and Richter (1981) are ~0.3 km/sec lower than our velocity-depth function.

Below 9-km depth, the laboratory results show that increasing temperature causes the velocity of quartz monzonite either to decrease slightly with increasing depth (high-geothermal gradient) or to remain essentially constant (lower geothermal gradient). However, both of our velocity models (Figures 5 and 7) have a positive velocity gradient in the lower crust which increases the velocity to 6.65 ± 0.15 km/sec at 25-km depth, ~0.3 km/sec higher than the velocity of the quartz monzonite

at that depth. Thus, as for the Diablo model, we suggest that a gradual compositional change causes a velocity increase as depth increases.

As previously explained, the lack of shear-wave data for the region limits the constraints that we can apply to the question of crustal composition. But if we restrict our discussion to only three possibilities, some useful statements can be made. Specifically, we ask whether the seismic data support a lower crust consisting of one of the following: mafic rocks (possibly oceanic crust); rocks of the Franciscan assemblage as suggested by Stewart (1968); or gneiss as suggested by Ross and McCulloch (1979).

We first consider the hypothesis that the Gabilan Range is underlain by mafic rocks of the same composition as the lower crust of the Diablo Range. A comparison of the crustal velocity structures (Figures 2 and 5) shows that above 15-km depth, the velocity in the Gabilan Range is higher than the velocity observed in the Diablo Range. Below 18 km, the velocity in the Gabilan Range is just at the lower estimate of the velocity in the Diablo Range. Although the velocity difference may be as little as 0.2 km/sec, we believe that it is resolvable and, therefore, conclude that it is unlikely that the two regions have the same lower crustal composition. If Franciscan rocks were present below 10-km depth in the Gabilan Range, we would expect the velocity to decrease to 5.9 to 6.1 km/sec, although we observe a velocity increase to 6.4 km/sec at that depth. Thus, we do not believe that Franciscan rocks underlie the Gabilan granites on a regional scale. The final possibility to be examined is that the lower crust changes from a granitic to a gneissic composition as depth increases. Ross (1978) has reported the mapped outcrops of high-grade gneiss on the flanks of the granite are probably the host rocks into which the granites were intruded at depth. The laboratory data provided by Kern and Richter (1981) show that the modeled velocities in the lower crust agree well with those measured for two gneiss samples and one amphibolite sample (Figure 10). On the basis of this evidence, a simple model for the Gabilan Range is a granitic upper crust underlain by a gneissic lower crust. Such a model is also consistent with the geologic evidence reviewed by Ross and McCulloch (1979), who proposed that gneissic rocks like those of the Santa Lucia Range directly underlie the Gabilan Range granites.

Our conclusion that the Gabilan Range is underlain by gneissic rocks bears on the models that invoke large lateral movements (500 to 2500 km) to bring the Salinian block to its present position between the Diablo Range and the Sur-Obispo terrane (Figure 1). If the gneissic lower crustal rocks detected seismically are the same as those mapped at near surface (Ross, 1978; Ross and McCulloch, 1979), then the upper crust has not been thrust over exotic country rock (e.g., Franciscan assemblage or oceanic crust), and the Salinian block has undergone lateral motion along a slip plane at or below the crust-mantle boundary. We emphasize that our data does not affect possible smaller, regional crustal thrusts within the Salinian block, whose faults would best be studied by reflection profiles.

LVZs in the Gabilan Range

In his interpretation of the Gabilan Range data, Stewart (1968) suggests that the range has an LVZ at 10-km depth that may be due to the presence of the Franciscan assemblage below granitic rocks at that depth. In view of the particular geologic importance of this suggestion, we discuss in some detail the seismic evidence for an LVZ.

The LVZ proposed by Stewart (1968) was based exclusively on the amplitude behavior of the first arrival data southeast from the San Juan shotpoint (Figure 6b).

The first arrival travel-time curve from this shotpoint begins with a velocity of 4.81 km/sec, increases to 6.06 km/sec at 12-km range, and then increases to 6.35 km/sec at 38-km range. Between 38 and 70 km, the 6.35 km/sec branch displays an amplitude decrease with increasing distance proportional to X^{-6}, where X is the distance from the shotpoint. This amplitude decrease, which is much stronger than the X^{-2} decrease associated with refracted waves, was the basis for Stewart's suggestion of the presence of an LVZ; the LVZ would produce a shadow effect that could explain the observed amplitude decrease.

We begin our discussion by emphasizing that Stewart's (1968) suggestion is a valid possibility, based on the observation he reports. However, there are alternative explanations. The 6.35 km/sec phase in question is unique to the San Juan record section (Figure 6b); this velocity is not observed on the reverse northwest profile from the shotpoint at Hernandez (Figure 6d), which is 74 km south of the San Juan shotpoint. This lack of consistency is bothersome; the case for an LVZ would be much stronger if the strong amplitude decrease were observed on the reverse profile. The fact that it is not suggests, as Stewart (1968) observes, that the decrease may be due to pronounced lateral structural changes in the upper few kilometers of the crust. For example, arrivals along an uptilted block would produce an apparent velocity of 6.35 km/sec; diffraction off the end of the block might be characterized by an amplitude decreases such as that observed here.

LVZs in the lower crust often can be identified on record sections on the basis of *PmP* reflection branches that do not asymptotically approach the intermediate refracted branches (*Pi*); the *PmP* reflection suffers a travel-time delay and the *Pi* refraction does not. Using the record section data from the Gabilan Range (Figure 6, a through e), we can compare the *PmP* branch to the *Pi* branch to see if they meet at large distances. The profile Big Basin southeast (Figure 6a) shows the *PmP* curve moves forward in reduced travel time, nearly meeting the intermediate refraction (layer 4) at a distance of 140 km. A very similar pattern is observed for the arrivals seen on the profile Ranchito northwest (Figure 6e); the *Pmp* curve moves forward in reduced travel time and arrives behind the intermediate refraction (*P*4) by 0.33 sec at 145 km, which indicates that the *PmP* curve will asymptotically approach the refracted branch at greater range. In conclusion, the evidence from reversed observations of deep crustal arrivals indicates that there is no substantial LVZ in the middle or lower crust of the Gabilan Range; instead the evidence indicates a gradual velocity increase as depth increases.

Summary

The ray-trace models derived from the record sections for the Diablo and Gabilan ranges confirm earlier suppositions that the crustal structure is different on opposite sides of the San Andreas fault (McEvilly, 1966; Stewart, 1968). The velocities in the upper crust of the Diablo Range (15 to 17.5 km thick) are no higher than 5.9 to 6.2 km/sec and indicate a crust composed of sediments and metasediments. The velocities in the upper crust of the Gabilan Range, which are no higher than 6.5 km/sec, are 0.3 km/sec higher than those of the Diablo Range at the same depth, because the crust of the Gabilan Range is composed of granitic rocks.

The lower crust of the Diablo Range (11.5 to 14.0 km thick) has a velocity of 6.5 to 7.0 km/sec, which indicates a mafic composition. Below 10-km depth, the velocity in the Gabilan Range may gradually increase with increasing depth from 6.35 to 6.55 km/sec without any velocity discontinuities, and this indicates a gneissic lower crust; alternatively, a 7- to 10-km thick lower crustal layer that has an average

velocity of 6.7 km/sec may exist below 16- to 19-km depth. Even with this layer, the velocity at a given depth appears to be slightly less than that of the Diablo Range, and this indicates that the contrast in crustal composition on either side of the San Andreas fault extends at least to the crust-mantle boundary. The depth to Moho is 24 to 26 km in the Gabilan Range and 26 to 30 km in the Diablo Range.

The disagreements between the observed and calculated travel times along both profiles indicate that the local velocity structure is more variable than the gross velocity structure presented above. Finer resolution of the velocity structure within the Diablo and Gabilan ranges, including the shear-wave velocities, requires the analysis of new refraction-profile, quarry-blast, and earthquake recordings.

ACKNOWLEDGMENTS

We are grateful to L. Baker, G. Maxwell, and J. Vinton for their assistance while we computed the ray-trace calculations on the USGS National Strong Ground Motion computer. We benefited during the course of this study from conversations and/or critical reviews by E. Banda, J. P. Eaton, E. R. Fluh, D. C. Ross, S. W. Stewart, and D. H. Warren. Editorial comments from D. Kruger and R. Rebello improved the text, and S. Cranswick drafted the figures.

REFERENCES

Bailey, E. H., W. P. Irwin, and D. L. Jones (1964). Franciscan and related rocks, and their significance in the geology of western California, *California Div. Mines and Geol. Bull.* **183,** 177.

Blümling, P. and C. Prodehl (1982). Crustal structure beneath the eastern part of the Coast Ranges (Diablo Range) of central California from explosion-seismic and near-earthquake data, *Tectonophysics* (in press).

Boore, D. M. and D. P. Hill (1973). Wave propagation characteristics in the vicinity of the San Andreas fault, in *Proceedings of the Conference on Tectonic problems of the San Andreas Fault System, Stanford Univ. Pub., Geol. Sci.* **13,** 215–224.

Byerly, P. (1939). Near earthquakes in central California, *Bull. Seism. Soc. Am.* **29,** 427–462.

Červený, V., I. A. Moltkov, and I. Psenčik (1977). Ray method in seismology, Univ. Karlova, Prague, 214 pp.

Champion, D. E., S. Gromme, and D. G. Howell (1980). Paleomagnetism of the Creataceous Pigeon Point Formation and the inferred northward displacement of the 2500 km for the Salinian block, California, *EOS, Trans. Am. Geophys. Union* **61,** 948.

Christensen, N. I. (1979). Compressional wave velocity in rocks at high temperatures and pressures: critical thermal gradients and crustal low velocity zones, *J. Geophys. Res.* **84,** 6849–6857.

Christensen, N. I. and D. M. Fountain (1975). Constitution of the lower continental crust based on experimental studies of seismic velocities in granulite, *Bull. Geol. Soc. Am.* **86,** 229–236.

Chuaqui, L. and T. V. McEvilly (1968). Detailed crustal structure within the central California large-scale seismic array, in *Annual Report,* Seismographic Station, University of California, Berkeley.

Dickinson, W. R. (1970). Relations of andesite, granites, and derived sandstone to arc-trench tectonics, *Rev. Geophys. Space Phys.* **8,** 813–860.

Eaton, J. P. and W. D. Mooney (1979). Coyote Lake earthquake traveltime patterns in central and southern California (abstract), *EOS, Trans. Am. Geophys. Union* **60,** 875.

Ernst, W. G. (1965). Mineral paragenesis of Franciscan metamorphic rocks, Panoche Pass, California, *Bull. Geol. Soc. Am.* **76,** 879–914.

Filson, J. (1970). *S* velocities at near distances in western central California, *Bull. Seism. Soc. Am.* **60,** 901–915.

Fuchs, K. and G. Müller (1971). Computation of synthetic seismograms and comparison with observations, *Geophys. J.* **23,** 417–433.

Hamilton, R. M., A. Ryall, and E. Berg (1964). Crustal structure southwest of the San Andreas fault from quarry blasts, *Bull. Seism. Soc. Am.* **54,** 67–77.

Healy, J. H. (1963). Crustal structure along the coast of California from seismic-refraction measurements, *J. Geophys. Res.* **68,** 5777–5787.

Healy, J. H. and L. G. Peake (1975). Seismic velocity structure along a section of the San Andreas fault near Bear Valley, California, *Bull. Seism. Soc. Am.* **65,** 1177–1197.

Jennings, C. W. and R. G. Strand (1958). Geologic map of California, Santa Cruz sheet, California Div. Mines and Geol., 1:250,000.

Kern, H. and A. Richter (1981). Temperature derivatives of compressional and shear wave velocities in crustal and mantle rocks at 6 Kbar confining pressure, *J. Geophys.* **49,** 47–56.

Lachenbruch, A. and J. H. Sass (1973). Thermo-mechanical aspects of the San Andreas fault system, *Proc. Conf. Tectonic Problems of San Andreas Fault System, Stanford Univ. Pub. Geol. Sci.* **13,** 192–205.

Levander, A. R. and R. L. Kovach (1981). *S*-wave observation in the Franciscan terrane, central California, *Bull. Seism. Soc. Am.* **71,** 1863–1874.

Lin, W. and C. Y. Wang (1980). *P*-wave velocities in rocks at high pressure and temperature and the constitution of the central California crust, *Geophys. J.* **61,** 379–400.

McEvilly, T. V. (1966). Crustal structure estimation within a large scale array, *Geophys. J.* **11,** 13–17.

Page, B. M. (1980). The southern Coast Ranges, in *Geotectonic Development of California,* W. G. Ernst, Editor, Prentice-Hall, New York, 329–417.

Prodehl, C. (1977). Record sections for selected local earthquakes recorded by the central California microearthquake network, *U.S. Geol. Surv., Open-File Rept. 77–37,* 310.

Prodehl, C. (1979). Crustal structure of the western United States, *U.S. Geol. Survey Profess. Paper 1034,* 74.

Rogers, T. H. (1966). Geologic map of California, San Jose sheet, California Div. Mines and Geol., 1:250,000.

Ross, D. C. (1978). The Salinian block-a Mesozoic granitic orphan in the California Coast Ranges, in *Mesozoic Paleogeography of the Western United States,* D. G. Howell and K. A. McDougall, Editors, Soc. Econ. Paleontologists and Mineralogists, Pacific Coast Paleogeography Symposium **2,** 559–573.

Ross, D. C. and D. S. McCulloch (1979). Cross section of the southern Coast Ranges and San Joaquin Valley from offshore of Point Sur to Madera, California, Geol. Soc. Am. Map and Chart Series MC-28H.

Steppe, J. A. and R. S. Crosson (1978). *P*-velocity models of the southern Diablo Range, California, from inversion of earthquake and explosion arrival times, *Bull. Seism. Soc. Am.* **68,** 357–367.

Stewart, S. W. (1968). Preliminary comparison of seismic traveltimes and inferred crustal structure adjacent to the San Andreas fault in the Diablo and Gabilan Ranges of central California, in *Proc. Conf. Geological Problems of San Andreas Fault System,* W. R. Dickinson and A. Grantz, Editors, *Stanford Univ. Pub. Geol. Sci.* **11,** 218–230.

Stewart, R. and L. Peselnick (1977). Velocity of compressional waves in dry Franciscan rocks to 8 kilobars and 300°C, *J. Geophys. Res.* **82,** 2027–2039.

Stewart, R. and L. Peselnick (1978). Systematic behavior of compressional velocity in Franciscan rocks at high pressure and temperature, *J. Geophys. Res.* **83,** 831–839.

Theilen, F. and R. Meissner (1979). A comparison of crustal and upper mantle features in Fennoscandia and the Rhenish shield, two areas of recent uplift, *Tectonophysics* **61,** 227–242.

Tocher, D. (1955). Seismic velocities and structure in northern California and Nevada, *Ph.D. Thesis,* Univ. of California, Berkeley, 120 pp.

Warren, D. H. (1978). Record sections of two seismic refraction profiles in the Gabilan and Diablo Ranges, California, *U.S. Geol. Surv., Open-File Rept. 78–340,* 12 pp.

Warrick, R. E., D. B. Hoover, W. H. Jackson, L. C. Pakiser, and J. C. Roller (1961). The specifications and testing of a seismic refraction system for crustal studies, *Geophysics* **26,** 820–824.

U.S. GEOLOGICAL SURVEY
345 MIDDLEFIELD ROAD, MS 77
MENLO PARK, CALIFORNIA 94025

Manuscript received 19 February 1982